Lattice dynamics and correlated atomic motion from the atomic pair distribution function

I.-K. Jeong,* R. H. Heffner, and M. J. Graf
Los Alamos National Laboratory, Los Alamos, New Mexico 87545

S. J. L. Billinge
Department of Physics and Astronomy and Center for Fundamental Materials Research, Michigan State University, East Lansing, Michigan 48824-1116

(Received 25 September 2002; published 18 March 2003)

The mean-square relative displacements (MSRD) of atomic pair motions in crystals are studied as a function of pair distance and temperature using the atomic pair distribution function (PDF). The effects of the lattice vibrations on the PDF peak widths are modelled using both a multi-parameter Born–von Karman (BvK) force model and a single-parameter Debye model. These results are compared to experimentally determined PDFs. We find that the near-neighbor atomic motions are strongly correlated, and that the extent of this correlation depends both on the interatomic interactions and crystal structure. These results suggest that proper account of the lattice vibrational effects on the PDF peak width is important in extracting information on static disorder in a disordered system such as an alloy. Good agreement is obtained between the BvK model calculations of PDF peak widths and the experimentally determined peak widths. The Debye model successfully explains the average, though not detailed, natures of the MSRDs of atomic pair motion with just one parameter. Also the temperature dependence of the Debye model largely agrees with the BvK model predictions. Therefore, the Debye model provides a simple description of the effects of lattice vibrations on the PDF peak widths.

DOI: 10.1103/PhysRevB.67.104301 PACS number(s): 63.20.−e, 61.12.−q, 61.10.−i

I. INTRODUCTION

The pair distribution function (PDF) obtained from the powder x-ray and neutron diffraction experiments has been shown to be of great value in determining the local atomic structure of materials.[1] The PDF results from a Fourier transform of the powder diffraction spectrum (Bragg peaks + diffuse scattering) into real-space.[2] For well ordered crystals, apart from technical details, this is similar to fitting the Bragg peaks + thermal diffuse scattering in the powder pattern in a manner first discussed by Warren.[3] A PDF spectrum consists of a series of peaks, the positions of which give the distances of atom pairs in real space. The ideal width of these peaks (aside from problems of experimental resolution) is due both to relative thermal atomic motion and to static disorder. Thus an investigation of the effects of lattice vibrations on PDF peak widths is important for at least two reasons: first, to establish the degree to which information on phonons (and the interatomic potential) can be obtained from powder diffraction data, and, second, to account for correlation effects in order to properly extract information on static disorder in a disordered system such as an alloy.

In general, powder diffraction is not considered a favorable approach for extracting information about phonons since, not only is energy information lost in the measurement, but also the diffuse scattering is isotropically averaged. The lattice vibrations are best described from the phonon dispersion curves determined using inelastic neutron scattering and high-energy-resolution inelastic x-ray scattering on single crystals.[4,5] Nevertheless, with the advent of high-energy synchrotron x-ray and pulsed-neutron sources and fast computers, it is possible to measure data with unprecedented statistics and accuracy. The PDF approach has been shown to yield limited information about lattice vibrations in powders,[6] though the extent of which this information can be extracted remains controversial.[7–10]

Measuring powders has the benefit that the experiments are straightforward and do not require single crystals. It is thus of great interest to characterize the degree to which lattice vibrations are reflected in the PDF using simple models, such as the Debye model, in situations where detailed interatomic potential information is not available. In this paper we explore these issues by comparing both measured PDFs and those calculated from realistic potential models with PDFs obtained through a single-parameter Debye model. This comparison is carried out as a function of atomic pair separation, temperature and direction in the lattice. We find that a single parameter Debye model explains much of the observed lattice vibrational effects on PDF peak widths, including the temperature dependence, in crystals like Ni, Ce, and GaAs. However, small but non-negligible deviations from the Debye model calculation are evident in crystal which needs a long-range interaction to explain anomalies in the dispersion curves.

II. CORRELATED ATOMIC MOTION IN REAL SPACE

The existence of interatomic forces in crystals results in the motion of atoms being correlated. This is usually treated theoretically by transforming the problem to normal coordinates, resulting in normal modes (phonons) that are non-interacting, thus making the problem mathematically tractible. Projecting the phonons back into real-space coordinates yields a picture of the dynamic correlations. This situation can be understood intuitively in the following way. Figure 1 shows a schematic diagram of atomic motion in three different interatomic force systems, each with its corresponding ideal PDF spectrum. In a rigid-body system [Fig. 1(a)], the

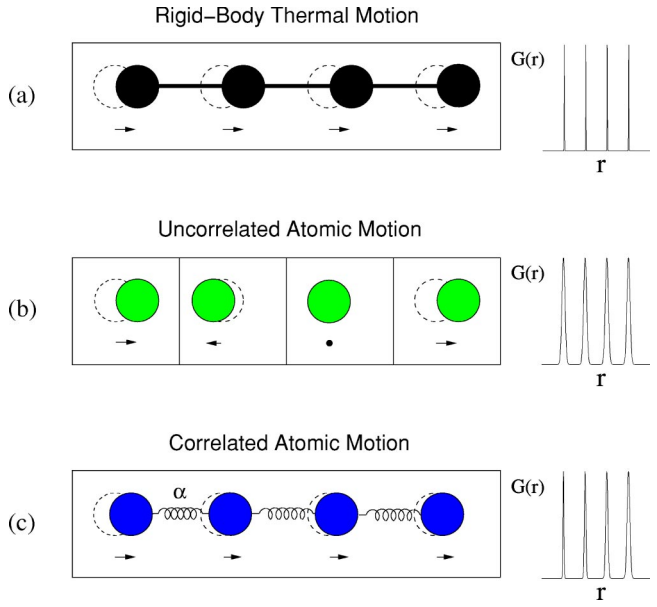

FIG. 1. (Color online) Schematic diagram showing an instantaneous snapshot of atomic positions in (a) a rigid-body model (b) an Einstein model, and (c) a Debye model. In (a) and (b) all PDF peaks have the same width independent of atom separation. In (c) the PDF peak width increases up to the root-mean-square displacement as the atomic separation increases. α is a spring constant.

interatomic force is extremely strong and all atoms move in phase. In this case, the peaks in the PDF are delta-functions. At the opposite extreme the atoms are non-interacting (the Einstein model) and move independently as shown in Fig. 1(b). This type of atomic motion results in broad PDF peaks whose widths are given by the root mean-square displacement amplitude ($\sqrt{\langle u^2 \rangle}$). In real materials, the interatomic forces depend on atomic pair distances, i. e., they are strong for nearest-neighbor interactions and get weaker as the atomic pair distances increase. In fact, these interactions are often quite well described with just nearest-neighbor or first- and second-nearest-neighbor coupling. The case of nearest-neighbor interactions is shown in Fig. 1(c). In this (Debye) model a single parameter corresponding to the spring constant of the nearest-neighbor interaction is used. Here, near-neighbor atoms tend to move in phase with each other, while far-neighbors move more independently. As a result, the near-neighbor PDF peaks are sharper than those of far-neighbor pairs. This behavior was first analyzed by Kaplow and co-workers in a series of papers[11–13] for a number of elemental metals.

III. EXPERIMENTS AND ANALYSIS

The experimental PDFs discussed here were measured using pulsed neutrons and synchrotron x-ray radiation. The neutron measurements were carried out at the NPD diffractometer at the Manual Lujan, jr., Neutron Scattering Center (LANSCE) at Los Alamos and the x-ray experiments at beam line A2 at CHESS (Cornell). Powder samples of Ni and a polycrystalline Ce rod were loaded into a vanadium can for the neutron measurements, carried out at room temperature. Powdered GaAs was placed between thin foils of kapton tapes for the x-ray measurements, measured at 10 K using 60 KeV ($\lambda = 0.206$ Å) x rays. Due to the higher x-ray energy at CHESS and relatively low absorption coefficient of GaAs, symmetric transmission geometry was used.

Both the neutron and x-ray data were corrected[14,15] for experimental effects and normalized to obtain the total scattering function $S(Q)$, using programs PDFgetN (Ref. 16) and PDFgetX,[17] respectively. The experimental PDF, $G(r)$, was obtained by taking the Fourier transform of $S(Q)$: $G(r) = 2/\pi \int_0^{Q_{max}} Q[S(Q)-1]\sin Qr dQ$, where Q_{max} is the maximum momentum transfer. The experimental PDF peak widths as a function of pair distance are extracted using the ''real-space'' Rietveld program PDFFIT.[18] For detailed procedures about modelling PDF spectrum and extracting PDF peak widths refer to Ref. 6

IV. MEAN-SQUARE RELATIVE DISPLACEMENTS IN CRYSTALS

In the harmonic approximation the PDF peak of simple materials can be well approximated by a Gaussian function with a width σ_{ij}.[19,20] The mean-square relative displacement of atom pairs, projected onto the vector joining the atom pairs, is given by

$$\sigma_{ij}^2 = \langle [(\mathbf{u_i} - \mathbf{u_j}) \cdot \hat{\mathbf{r}}_{ij}]^2 \rangle, \tag{1}$$

where $\mathbf{u_i}$ and $\mathbf{u_j}$ are thermal displacements of atoms i and j from their average positions.[19,20] The vector $\hat{\mathbf{r}}_{ij}$ is a unit vector parallel to the vector connecting atoms i,j, and the angular brackets indicate an ensemble average. This equation can be rearranged as

$$\sigma_{ij}^2 = \langle [\mathbf{u_i} \cdot \hat{\mathbf{r}}_{\mathbf{ij}}]^2 \rangle + \langle [\mathbf{u_j} \cdot \hat{\mathbf{r}}_{\mathbf{ij}}]^2 \rangle - 2\langle (\mathbf{u_i} \cdot \hat{\mathbf{r}}_{\mathbf{ij}})(\mathbf{u_j} \cdot \hat{\mathbf{r}}_{\mathbf{ij}}) \rangle. \tag{2}$$

Here the first two terms correspond to mean-square thermal displacement of atoms i and j. The third term is a displacement correlation function, which carries information about the motional correlations. For a monatomic crystal, the σ_{ij}^2 is expressed in terms of the phonons as follows:[20]

$$\sigma_{ij}^2 = \frac{2\hbar}{NM} \sum_{\mathbf{k},s} \frac{(\hat{\mathbf{e}}_{k,s} \cdot \hat{\mathbf{r}}_{ij})^2}{\omega_s(\mathbf{k})} \left[n(\omega_s(\mathbf{k})) + \frac{1}{2} \right] [1 - \cos(\mathbf{k} \cdot \mathbf{r_{ij}})], \tag{3}$$

where $\omega_s(\mathbf{k})$ is a phonon frequency with wave vector $\mathbf{k}$ in branch s, $n(\omega_s(\mathbf{k}))$ is a phonon occupation number, $\hat{\mathbf{e}}_{k,s}$ is a polarization vector of the $\mathbf{k},s$ phonon mode, N is the number of atoms and M is the mass of an atom. As an example, we calculate the σ_{ij}^2 of Ce (Fig. 2) using Eq. (3). Ce (γ-phase) crystallizes in a simple fcc structure (space group Fm3m) at room temperature and atmospheric pressure.[21] In this calculation, the phonon frequency ($\omega_s(\mathbf{k})$) and the polarization vector ($\hat{\mathbf{e}}_{k,s}$) were obtained by solving the dynamical matrix using up to the eighth nearest-neighbor (NN) interatomic force parameters. The force parameters of Ce were determined by Stassis *et al.*[22] by fitting phonon dispersion curves using the Born-von Karman (BvK) model.[23] In Fig. 2 the

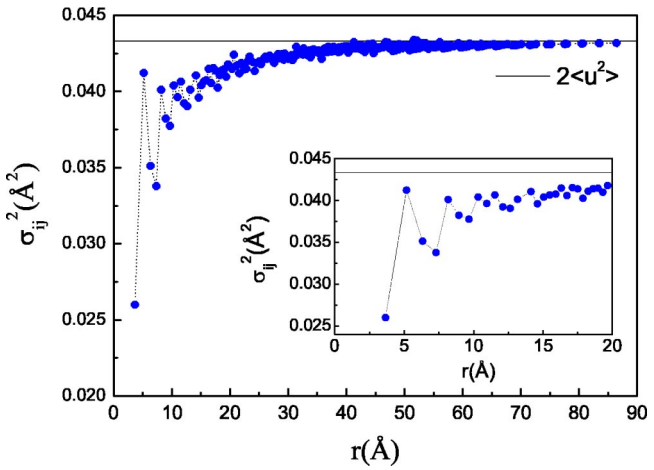

FIG. 2. (Color online) Theoretical mean-square relative displacement σ_{ij}^2 of γ-Ce as a function of pair distance calculated using Eq. (3) and the BvK model at 300 K. The inset shows σ_{ij}^2 below $r_{ij} \leqslant 20$ Å. The solid line corresponds to $2\langle u^2 \rangle$, where $\langle u^2 \rangle$ is the mean-square thermal displacement of γ-Ce.

horizontal solid line corresponds to $2\langle u^2 \rangle$, where $\langle u^2 \rangle$ is the mean-square thermal displacement of Ce. Deviations from this line are due to motional correlations in the pair motion. The inset shows σ_{ij}^2 below $r_{ij} \leqslant 20$ Å, where the motional correlation is more apparent. Evidently, motion of near-neighbor atoms is highly correlated, and this is reflected in narrower PDF peak widths. At larger separations ($r_{ij} \geqslant 20$ Å) the σ_{ij}^2 values asymptotically approach the uncorrelated values because the cosine term in Eq. (3) averages to zero.

As shown in Fig. 2, the motional correlation of atom pairs varies significantly as a function of pair distance. Therefore it is useful to quantify the degree of correlation using a dimensionless correlation parameter ϕ which can be defined as:[24,6]

$$\sigma_{ij}^2 = \sigma_i^2 + \sigma_j^2 - 2\sigma_i \sigma_j \phi, \tag{4}$$

where $\sigma_i^2 = \langle (\mathbf{u_i} \cdot \hat{\mathbf{r}}_{\mathbf{ij}})^2 \rangle$. It can be seen from Eq. (4) that $\phi = 0$ corresponds to completely uncorrelated motion. Positive values of ϕ describe a situation where the atoms move in phase, and thus the resulting value of σ_{ij} is smaller than for the uncorrelated case. Using Eq. (4) the correlation parameter ϕ can be calculated from the PDF peak width measurements as

$$\phi = \frac{(\sigma_i^2 + \sigma_j^2) - \sigma_{ij}^2}{2\sigma_i \sigma_j}. \tag{5}$$

Figure 3 shows the motional correlations along various crystallographic directions in Ce. It is clear that the correlation parameter varies significantly with crystallographic direction. Along the $\langle 110 \rangle$ direction, Ce atomic motion shows strong correlation. On the other hand, Ce atoms along $\langle 100 \rangle$ show almost no motional correlation. This behavior comes principally from the characteristic elastic anisotropy of cubic crystals.[25] Despite the extensive orientational averaging of the powder measurement, this directional information survives in the data.

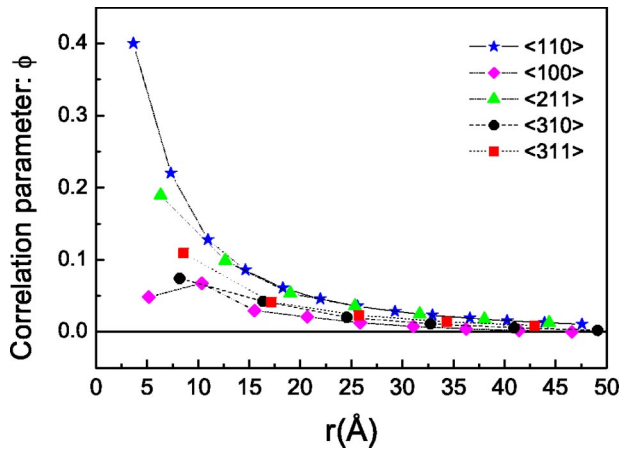

FIG. 3. (Color online) Correlation parameter ϕ of Ce atoms along various crystallographic directions obtained using the BvK model calculations at 300 K. $\phi = 0$ corresponds to the uncorrelated atomic motion, and $\phi > 0$ indicates that atoms move in phase.

The oscillations in σ_{ij}^2 shown in Fig. 2 for Ce are generally driven by both the interatomic interactions and the crystal structure. This is illustrated in Figs. 4 and 5, which show the correlation parameter ϕ for a variety of fcc and bcc materials. The σ_{ij}^2 in Figs. 4 and 5 are generated in the same way as for Ce, that is, using the BvK force model, with parameters derived from fits to the phonon dispersion curves found in the literature.[26] One sees that a common oscillatory behavior in the correlation parameter is found for all of the fcc crystals studied. And similar but distinct oscillatory features are observed for the bcc crystals, except Nb. This difference in the general behavior of fcc and bcc crystals suggests that atomic geometry plays a role in the motional correlations as well as the interatomic interaction. However, significant differences in the correlation are evident among different elements with the same crystal structure as well. For example, in fcc crystals ϕ varies from 0.37 to 0.45 for the 1NN pair and from 0.05 to 0.2 for the 2NN pair. In bcc

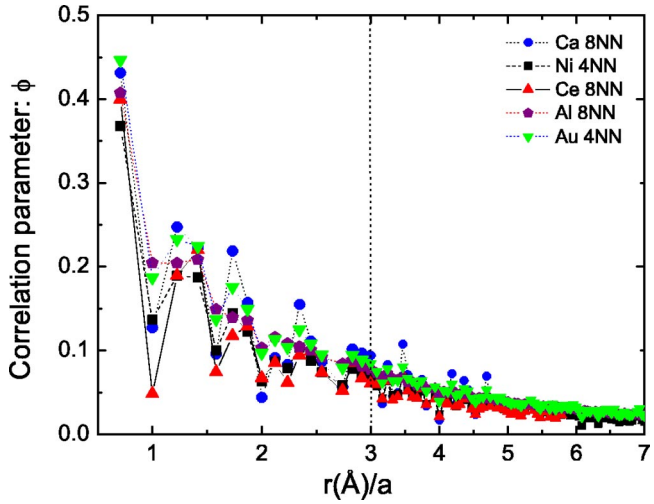

FIG. 4. (Color online) Correlation parameter ϕ of fcc crystals Ca, Ni, Ce, Al, and Au at 300 K, obtained using the BvK model calculations. **a** is the lattice parameter of each crystal.

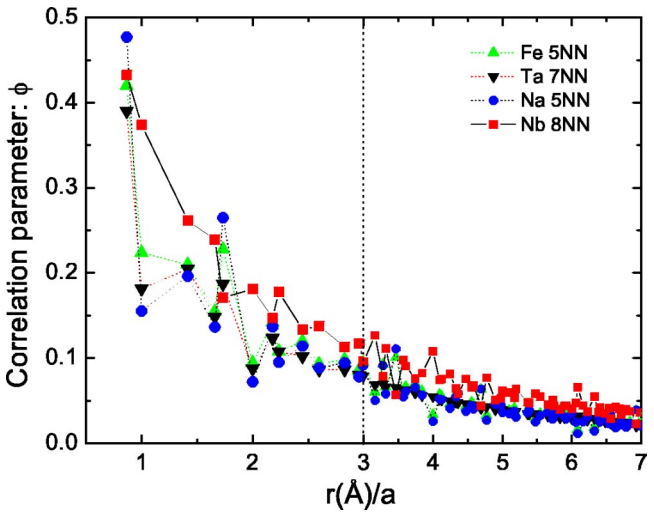

FIG. 5. (Color online) Correlation parameter ϕ of bcc crystals Fe, Ta, Na, and Nb at 300 K, obtained using the BvK model calculations. **a** is the lattice parameter of each crystal.

crystals ϕ varies from 0.38 to 0.47 for the 1NN pair. Thus, ϕ and σ_{ij}^2 do reflect interatomic interactions.

In addition to a dependence on the atom pair distance r_{ij}, the σ_{ij}^2 shows an explicit dependence on phonon frequencies $\omega_k(s)$. Therefore, it is instructive to consider how phonon modes of different frequencies contribute to the broadening of the peak widths. Figure 6 shows the frequency spectrum of σ_{ij}^2 in Ce for the 1NN, 2NN, and 10NN peaks, in addition to that of the uncorrelated far-neighbor atom pairs. Referring to Fig. 6, for the 1NN, the low frequency ($\omega/2\pi \leqslant 1$ THz) thermal motion contributes little to the 1NN PDF peak width broadening. Most of the peak broadening comes from mid-to-high frequency modes ($1 \leqslant \omega/2\pi \leqslant 2.8$ THz), which contribute almost equally to the broadening. This suggests that 1NN pair moves more or less in-phase at low frequencies, and that the pair motion de-phases somewhat as the frequency increases. For the 2NN and higher-neighbors peaks, however, where the motion of atom pairs gets more and more de-phased as the pair distance increases, the medium-range frequency modes predominantly contribute to peak width broadening. Finally, for the far-neighbor atom pairs, where the motion is completely uncorrelated, the frequency spectrum is spread more evenly across all of the frequencies.

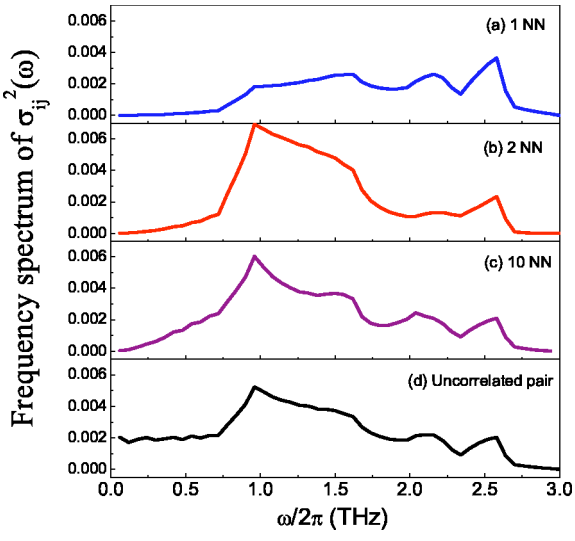

FIG. 6. (Color online) Frequency spectrum of σ_{ij}^2 for Ce at 300 K obtained using the BvK model calculations: (a) 1NN, (b) 2NN, (c) 10NN, and (d) uncorrelated far-neighbor atom pair. The area underneath the solid line in each figure corresponds to the σ_{ij}^2 of each pair.

V. CORRELATED THERMAL MOTION: DEBYE APPROXIMATION

Using the BvK model we have shown that near-neighbor atomic motions in crystalline materials are strongly correlated. In the BvK model calculation, however, the force constants must be known in advance. In this section, we simplify the result in Eq. (3) using some approximations to describe the effects of the lattice vibrations on the PDF peak widths without knowing the force constants. Following Debye[27] and Beni and Platzmann,[28] we make no distinction between longitudinal and transverse phonon modes and take a spherical average. Then Eq. (3) reduces to

$$\sigma_{ij}^2 = \left\langle \frac{2\hbar}{M\omega}\left[n(\omega)+\frac{1}{2}\right][1-\cos(\mathbf{k}\cdot\mathbf{r_{ij}})]\right\rangle, \tag{6}$$

where $\langle\cdots\rangle$ is the average over the $3N$ modes and N is the number of atoms. This result is a general expression for all materials and is independent of the number of atoms per unit cell.[25] Using the Debye approximation, $\omega = ck$, we can write Eq. (6) as[29]

$$\sigma_{ij}^2 = \frac{2\hbar}{3NM}\int_0^{\omega_D} d\omega \frac{\rho(\omega)}{\omega}\left[n(\omega)+\frac{1}{2}\right]\left[1-\frac{\sin(\omega r_{ij}/c)}{\omega r_{ij}/c}\right], \tag{7}$$

where $\rho(\omega) = 3N(3\omega^2/\omega_D^3)$ is the phonon density of states, $n(\omega)$ is the phonon occupation number, c is the sound velocity and $\omega_D = ck_D$ is the Debye cutoff frequency. The Debye wavevector is given by $k_D = (6\pi^2 N/V)^{1/3}$ where N/V is the number density of the crystal. After integrating over ω, we obtain

$$\sigma_{ij}^2 = \frac{6\hbar}{M\omega_D}\left[\frac{1}{4}+\left(\frac{T}{\Theta_D}\right)^2\Phi_1\right] - \frac{6\hbar}{M\omega_D}\left[\frac{1-\cos(k_D r_{ij})}{2(k_D r_{ij})^2} + \left(\frac{T}{\Theta_D}\right)^2\int_0^{\Theta_D/T} x\,\frac{\sin\left(\frac{k_D r_{ij} T x}{\Theta_D}\right)\Big/\left(\frac{k_D r_{ij} T}{\Theta_D}\right)}{e^x-1}\,dx\right], \tag{8}$$

where $\Phi_1 = \int_0^{\Theta_D/T} x(e^x-1)^{-1}dx$, x is a dimensionless integration variable and Θ_D ($=\hbar\omega_D/k_B$) is the Debye temperature. This result is known as the "correlated Debye (CD) model".[28,30,29] Here, the first term corresponds to the usual uncorrelated mean-square thermal displacements ($2\langle u^2\rangle$) and the second term is a displacement correlation function

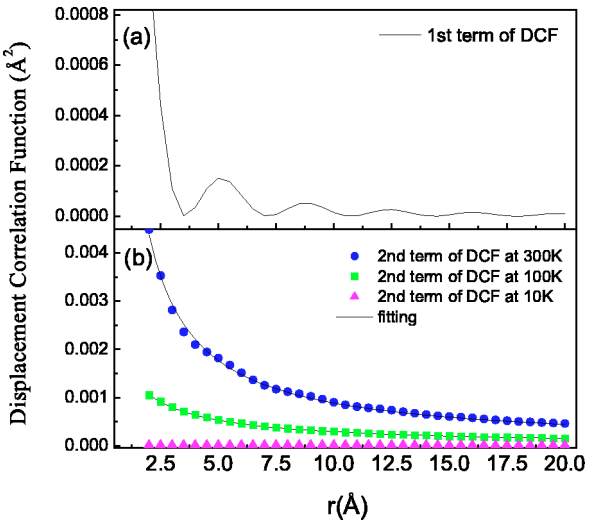

FIG. 7. (Color online) Displacement correlation function (DCF) of Ni. (a) The first term of the DCF of Eq. (8). (b) The second term of the DCF of Eq. (8) at 300, 100, and 10 K. The solid line is a fit to a $1/r$ dependence.

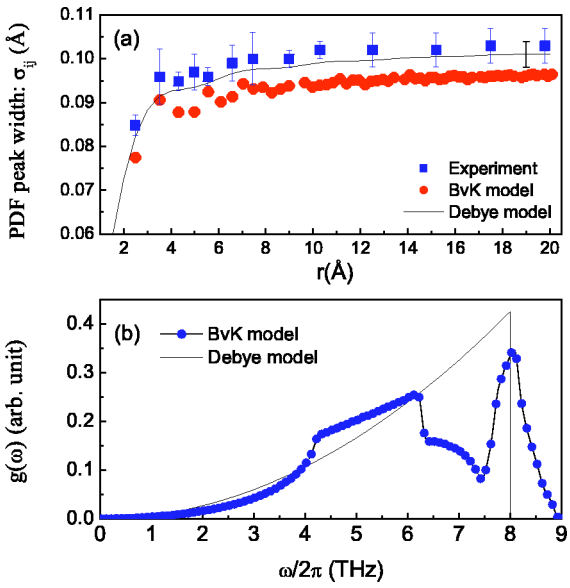

FIG. 8. (Color online) (a) Comparison of neutron PDF and BvK model peak widths with those of the CD model calculation of Ni at 300 K. Filled squares: experimental PDF peak widths (only a few selected peak widths are shown), Filled circles: BvK model calculations. Dotted line: CD model calculation using Debye temperature $\theta_D = 385$ K, and Debye wave vector $k_D = 1.756$ Å^{-1}. (b) Solid line: Ni phonon density of states calculated using BvK model. Dotted line: Debye density of states with the same area as the BvK calculation. Debye cutoff frequency $\omega_D/2\pi = 8$ THz.

(DCF). The CD model was first used to explain x-ray absorption fine structure (XAFS) peak widths as a function of temperature, and provided reasonable fits to the 1NN and 2NN peak widths. However, this model has never been tested beyond the 2NN peak. Here we test this simple model against full experimental PDF spectra and the BvK model calculations.

In the CD model the DCF shows explicit dependence on the atomic pair distance r_{ij}. The first term of the DCF comes from the quantum zero-point motion and the second term is temperature dependent. Figure 7 shows the r_{ij} dependence of the first and second terms of the DCF of Ni. The first term of the DCF decreases as $1/r_{ij}^2$ with a cosine modulation. The second term is temperature dependent and shows a $1/r_{ij}$ dependence. At low temperatures ($T \ll \theta_D$), the temperature dependent DCF term is much smaller than the zero-point motion term. However, as the temperature increases the second term becomes dominant. These results show that the motional correlation follows a $1/r_{ij}^2$ dependence when $T \ll \theta_D$ and a $1/r_{ij}$ when $T \geqslant \theta_D$.

We tested the CD model calculation against the experimental and BvK PDF peak widths of Ni at 300 K. Figure 8 shows selected experimental PDF peak widths and the calculated peak widths as a function of pair distance, as well as the corresponding phonon density of states of Ni. The errors in the experimental PDF peak widths were estimated from fitting Gaussian functions to the PDF peaks. The error in CD model calculation was estimated from the error in the experimental thermal displacement. For the BvK model calculation, we used up to the 4th NN force parameters determined by Birgeneau *et al.*[31] We also compared the 4NN BvK model calculations with those of a simple 1NN BvK model and found excellent agreement between them. Our experimental thermal displacement of Ni ($\langle u^2 \rangle = 0.00535$ Å^2) is about 10% larger than that of the BvK model calculation. As a result, as shown in Fig. 8(a), the BvK model peak widths are shifted downward by roughly 5% overall. The origin of this difference between our thermal displacement and that of the BvK calculation is not clear but the Debye temperature, determined from our thermal displacement using the Debye approximation, $\theta_D = 385$ K, compares well to the specific heat measurement, where $\theta_D = 375$ K.[32] For the CD model calculation the Debye wave vector $k_D = 1.756$ Å^{-1} was obtained from the atomic geometry. The only parameter in the CD model, the Debye temperature, was determined from the experimental thermal displacement.

As shown in Fig. 8(b), the Debye model reasonably approximates the "real" density of states in this simple element. However, because the Debye temperature and corresponding Debye frequency were obtained from the thermal displacement, and not from the sound velocity, the low-frequency Debye density of states deviates from those of the BvK model by roughly 15%. Nevertheless, the CD model calculation of the peak widths shows good agreement with the experimental PDF peak widths σ_{ij} except for the overall downward shift.

We now move to the more complex case of Ce, which needs long-range forces to explain anomalies in the dispersion curves. Up to the eighth NN interactions are required to reasonably fit the phonon dispersion curves of Ce.[22] Figure 9 shows selected experimental PDF peak widths and calculated peak widths as a function of pair distance, as well as the phonon density of states of Ce. In this case, the BvK calculation of the peak widths shows a good agreement with the experimental PDF peak widths. We also found that a simple 1NN BvK model calculation shows very good overall agree-

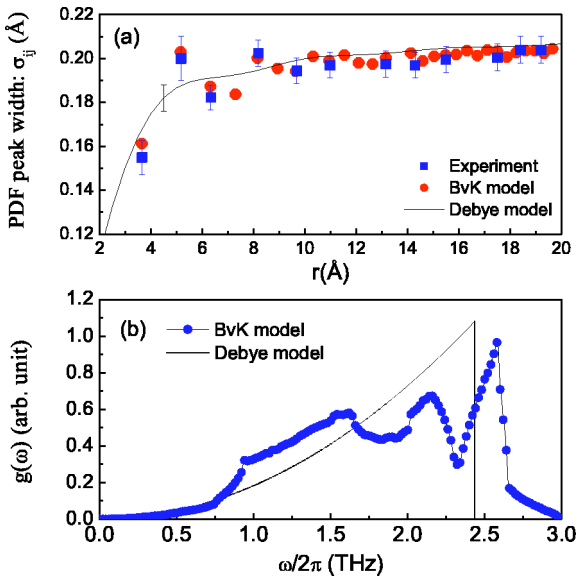

FIG. 9. (Color online) (a) Comparison of neutron PDF and BvK model peak widths with those of the CD model calculation of Ce at 300 K. Filled squares: experimental PDF peak widths (only a few selected peak widths are shown), Filled circles: BvK model calculation. Dotted line: CD model calculation with Debye temperature $\theta_D=117$ K and Debye wave vector $k_D=1.1986$ Å^{-1}. (b) Solid line: Ce phonon density of state calculated using the BvK model. Dotted line: corresponding Debye density of states, using a Debye cutoff frequency $\omega_D/2\pi=2.44$ THz.

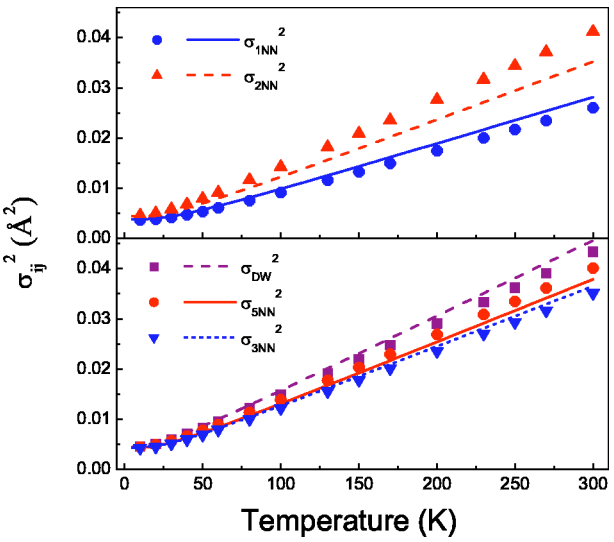

FIG. 10. (Color online) Mean-square relative displacement σ_{ij}^2 of Ce as a function of temperature. Upper panel: nearest neighbor (NN), second NN (2NN). Lower panel: third NN (3NN), fifth NN (5NN), and DW. DW represents an uncorrelated far-neighbor pair. Symbols are the Born von-Karman (BvK) model calculations and lines are the corresponding CD model calculations. In BvK calculation, the Debye temperature $\theta_D=117$ K is determined at 300 K.

ment with that of 8NN BvK model, except for the 2NN PDF peak width which deviates by ~3%. For the CD model calculation, a Debye wavevector $k_D=1.1986$ Å^{-1} and a Debye temperature $\theta_D=117$ K (at 300 K) were obtained from the atomic geometry and thermal displacement of Ce ($\langle u^2\rangle=0.0231$ Å^2), respectively. Even for the more complex system like Ce, the CD model calculation of the PDF peak widths reproduces the overall r_{ij}-dependence rather well, except for a few detailed features.

We now consider in the harmonic approximation the hypothetical (assuming no phase transition) T-dependence of σ_{ij}^2 for Ce atom pairs to compare the CD model with the BvK model. These are shown in Fig. 10 for the first few NN pairs, as well as the uncorrelated atom pair. All of these curves exhibit characteristic Debye-like behavior, i.e., linearity in T at high temperatures, but curving over to a common zero-point value at $T=0$. In general, the CD model calculation of the temperature dependence of the σ_{ij}^2 shows good agreement with that of the BvK model calculation, except for the 2NN pair (Fig. 10). Referring to Fig. 9 we see that BvK calculations of the σ_{ij}^2 of the 1NN and 3NN lie very close to the Debye prediction, but the 2NN is displaced significantly upwards. The deviations between the BvK and Debye models increase as the temperature increases. Apparently, if the σ_{ij}^2 lies on the Debye prediction at one temperature, the Debye model will also predict its temperature dependence correctly. Conversely, the temperature dependence of σ_{ij}^2 will be underestimated or overestimated depending on whether it is displaced above or below the Debye curve at the lowest temperatures, respectively. This is at least true for Ce.

As a final example, we compare the CD model calculation of PDF peak widths with those of GaAs determined experimentally. This is distinct from the above examples due to the presence both of more than one atomic species and directional covalent bonding. We also compare the CD model calculation with a lattice-dynamics calculation using the Kirkwood potential, which has been shown to be a good basis for describing semiconductor compounds and alloys.[33,15] Figure 11(a) shows the atom pair dependence of the PDF peak widths of GaAs at 10 K. In the Kirkwood model, the potential parameters are obtained by fitting the nearest and far neighbor PDF peak widths.[33,15] In Fig. 11(a), the Kirkwood model calculation using bond stretching ($\alpha=96$ N/m) and bending ($\beta=10$ N/m) force constants shows quite good agreement with the experimental PDF peak widths. In the CD model, the average mass of Ga and As is used. The Debye wavevector $k_D=1.382$ Å^{-1} and Debye temperature $\theta_D=250$ K were obtained from the atomic geometry and by fitting the far-neighbor PDF peak widths. In the CD model calculation, the near-neighbor peaks ($r\leqslant 5$ Å) are ~10% broader than those of the experimental peaks. Referring to Fig. 11(b), the Debye model does a poor job of describing the GaAs phonon density of states; for example, the high frequency optic modes, $6\leqslant\omega/2\pi\leqslant 8$ THz, are totally missed. Instead, the Debye model overestimates phonon modes between 3.5 THz$\leqslant\omega/2\pi\leqslant\omega_D$. This poor description of the phonon density of states, as well as the use of the average mass of Ga and As for M in Eq. (7), leads to deviations in near-neighbor peak widths from those of the experimental peaks and the BvK model calculations. Therefore, the deviations in CD model calculations basically reflect the limitation of the CD model in describing motional correlations in a system with optic modes. Nevertheless, the

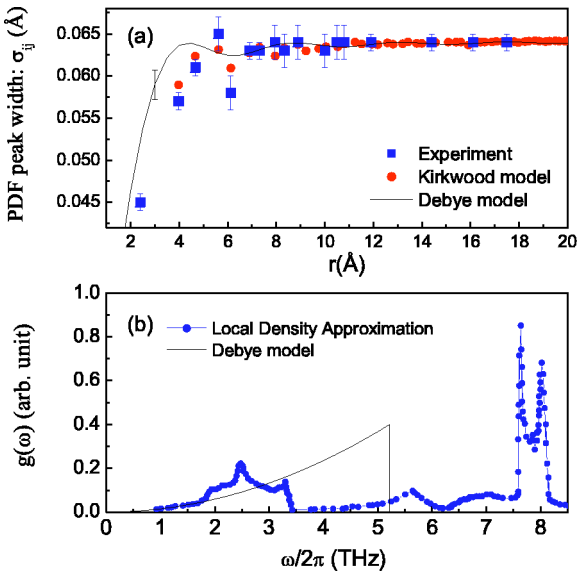

FIG. 11. (Color online) (a) PDF peak widths of GaAs as a function of atom separation at 10 K. Filled squares: experimental x-ray PDF peak widths. Filled circles: lattice dynamics calculation using the Kirkwood model ($\alpha=96$ N/m, $\beta=10$ N/m). Dotted line: CD model calculation using the Debye temperature $\theta_D=250$ K and Debye wave vector $k_D=1.382$ Å^{-1}. (b) Symbols: GaAs phonon density of states calculated using the local-density approximation density functional theory (Ref. 41). Solid line: Debye density of states with the same area as the local-density-approximation calculation. Debye cutoff frequency $\omega_D/2\pi=5.22$ THz.

CD model, with a single parameter θ_D determined from the thermal displacement, serves as a good first order approximation to the PDF peak widths, even in more complex systems like GaAs.

So far we neglected anharmonicity in our quasiharmonic analysis. However, this simplification has no consequences on our conclusions. In general, anharmonic corrections to the Debye-Waller factor and PDF peaks are important near the melting transition or structural phase transitions.[34–37] In simple materials these corrections are small, e.g., in γ-Ce, following the work by Maradudin and Flinn,[34] we estimate the correction to the harmonic Debye-Waller factor to be order of one percent at room temperature. Such a small correction is well within the current experimental uncertainties and difficult to extract from measurements. In fact, γ-Ce and Th-doped Ce are well described by the harmonic approximation of the interatomic potentials.[38,39] An exception is Pb, which shows large anharmonic corrections in the Debye-Waller factor ($\sim$9% at room temperature). Here we expect to observe similar large corrections in measured PDF peaks as a function of temperature. Thus in the future it will be possible to model and extract anharmonic contributions from the atomic pair-distribution function.

VI. DISCUSSION

The mean-square relative displacements σ_{ij}^2 and the corresponding correlation parameter shown in Figs. 2, 4, 5, 8, and 9 present two interesting pieces of information about the atomic motions in a crystalline material. First of all, they show that nearest-neighbor atomic motion is significantly correlated. Second, the details of the motional correlations as a function of pair distance display structures which deviate from the predictions of the simple CD model. Here we can raise some interesting questions. How is this structure in the motional correlation of atom pairs related to the underlying interatomic potentials? Can one extract the potential parameters using an inverse approach to model the PDF peak widths with the potential parameters as input?

Reichardt and Pintschovius[8] argued that the calculated PDF peak widths as a function of pair distance are rather insensitive to the details of the lattice dynamics models used to calculate σ_{ij}^2. They found that PDFs calculated using either very simple or complex models didn't show significant differences. A similar conclusion has been reached by Graf *et al.*,[10] in contradiction to previous claims by Dimitrov *et al.*[7] Indeed, the magnitude of errors implicit in the measurement and data analysis appear to be comparable to the effects that must be measured to obtain quantitatively accurate potential information using this approach.[9] The conclusions of Reichardt and Pintschovius and Graf *et al.* and Thorpe *et al.* are largely borne out by the present work; e.g., the grossly oversimplified CD model, which neglects elastic anisotropy and parameterizes the dynamics with a single number θ_D, is rather successful at explaining the smooth r_{ij} dependence of the PDF peak widths.

Thus, when the BvK force parameters are not available, we have shown that the correlated Debye (CD) model is a reasonable approximation to describe both the smooth r_{ij}-dependence and the temperature dependence of σ_{ij}^2 in simple elements. Considering the poor correspondence between the Debye phonon density of states and the BvK density of states, the reasonable agreement between the BvK model calculations of σ_{ij}^2 and that of the CD model is rather surprising. This confirms that the PDF peak width is rather insensitive to the details of the phonon density of states and the phonon dispersion curves, as suggested by Reichardt and Pintschovius and by Graf *et al.* Any information about the interatomic forces in the PDF peak widths is contained in the small deviations of the σ_{ij}^2 from those of the CD model calculations. Therefore, extracting interatomic potential information from the PDF peak widths is unlikely. However, these deviations could possibly yield some average phonon information. For example, recent calculations by Graf *et al.*[10] showed that one can obtain phonon moments within a few percent accuracy for most fcc and bcc crystals using the nearest-neighbor force parameters extracted from a theoretical BvK PDF spectrum. This result indicates that the PDF spectrum contains some average phonon information, although it doesn't provide detailed phonon dispersion information. The average phonon information, such as phonon moments from the PDF peak widths, will be a useful complement to optical and acoustic techniques that yield zone-center information in situations where single crystal measurements are not possible. This complementarity also extends to the extraction of Debye-Waller factors from powder diffraction measurements.

Finally, a comparison of the CD model calculations of the

PDF peak widths in GaAs with those of experimental PDF and Kirkwood model calculations shows additional limitations of the CD model. In the CD model calculation, the near-neighbor PDF peaks below $r \leqslant 5$ Å are about 5–10 % broader than those of experimental PDF peaks. This is due to the poor description of GaAs phonon density of states by the Debye model. Since the sine term in Eq. (7) over- and underweighs certain phonon modes depending on their frequencies, the redistribution of GaAs phonon density of states in a realistic model causes deviations in near-neighbor peak widths from those of the CD model. One way to improve the model calculation in materials which have optic modes might be a hybrid model that combines the correlated Debye and Einstein models. Such a hybrid model has worked quite well in the case of AgI.[40]

VII. SUMMARY

In this paper the mean-square relative displacements (σ_{ij}^2) of atomic pair motion in crystals have been studied as a function of pair distance and temperature using the atomic pair distribution function (PDF). The experimental PDF peak width and the BvK model calculations of σ_{ij}^2 as a function of pair distance show that the near-neighbor atomic motions are strongly correlated. The extent of these correlations depends both on the interatomic interactions and crystal structure. Thus a proper accounting of the lattice vibrational effects on the PDF peak widths is important in order to better understand the effects of static and dynamic disorder on the PDF peak widths in disordered systems. Details of the PDF peak widths vs r_{ij} seen in the BvK calculations are well reproduced in the measured data indicating the accuracy of the measurements. Most of these details originate from the elastic anisotropy of the crystal which is especially apparent in fcc crystals. We showed that the CD model reproduces the average features of the lattice vibrational effects on the PDF peak width with just one parameter, which is determined from the measured thermal displacement $\langle u^2 \rangle$. Therefore, this simple model can be used as an important adjunct when using PDF to extract static and dynamic disorder information from materials with local lattice distortion. In addition, the T dependence of the CD model largely agrees with the BvK model calculations. Good agreement between CD model and experimental PDF peak widths indicates that the PDF peak widths are rather insensitive to the details of phonon density of states and the phonon dispersion curves. Any information about the interatomic forces in the PDF peak widths is contained in the small deviations ($\leqslant 5\%$) of the σ_{ij} from those of the CD model calculation. This makes the extraction of interatomic potential information from PDF peak widths alone unlikely.

ACKNOWLEDGMENTS

I.K.J. gratefully acknowledges Professor M. F. Thorpe for many helpful discussions. We thank Dr. T. Darling, Dr. Th. Proffen, and Dr. A. C. Lawson for the help with the data collections. S.J.L.B. acknowledges support from the U.S. Department of Energy, Office of Science, through Grant No. DE-FG02-97ER45651. Works by I.K.J., M.J.G., and R.H.H. were carried out under the auspices of the U.S. Department of Energy, Office of Science. Part of the data were collected at the Manuel Lujan, Jr. Neutron Scattering Center which is a national user facility funded by the U.S. Department of Energy, Office of Basic Energy Sciences. Part of this work was based upon research conducted at the Cornell High Energy Synchrotron Source (CHESS), which is supported by the National Science Foundation and the National Institutes of Health/National Institute of General Medical Sciences under award DMR 9713424.

*Electronic address:
jeong@lanl.gov; URL: http://www.totalscattering.org/

[1] *Local Structure from Diffraction*, edited by S. Billinge and M. F. Thorpe (Plenum, New York, 1998).
[2] T. Egami, in *Local Structure from Diffraction*, edited by S. J. L. Billinge and M. F. Thorpe (Plenum, New York, 1998), p. 1.
[3] B. E. Warren, Acta Crystallogr. **6**, 803 (1953).
[4] M. Schwoerer-Bohning, A. T. Macrander, and D. Arms, Phys. Rev. Lett. **80**, 5572 (1998).
[5] T. Ruf, J. Serrano, M. Cardona, P. Pavone, M. Pabst, M. Krisch, M. D'Astuto, T. Suski, I. Grzegory, and M. Leszczynski, Phys. Rev. Lett. **86**, 906 (2001).
[6] I.-K. Jeong, Th. Proffen, F. Mohiuddin-Jacobs, and S. J. L. Billinge, J. Phys. Chem. A **103**, 921 (1999).
[7] D. A. Dimitrov, D. Louca, and H. Röder, Phys. Rev. B **60**, 6204 (1999).
[8] W. Reichardt and L. Pintschovius, Phys. Rev. B **63**, 174302 (1999).
[9] M. F. Thorpe, V. A. Levashov, M. Lei, and S. J. L. Billinge, *From Semiconductors to Protein: Beyond the Average Structure* (Plenum, New York, 2002), pp. 105–128.
[10] M. J. Graf, I.-K. Jeong, D. L. Starr, and R. H. Heffner, cond-mat/0209540 (unpublished).
[11] R. Kaplow, B. L. Averbach, and S. L. Strong, J. Phys. Chem. Solids **25**, 1195 (1964).
[12] R. Kaplow, S. L. Strong, and B. L. Averbach, Phys. Rev. **138**, 1336 (1965).
[13] R. Lagneborg and R. Kaplow, Acta Metall. **15**, 13 (1967).
[14] S. J. L. Billinge and T. Egami, Phys. Rev. B **47**, 14 386 (1993).
[15] I.-K. Jeong, F. Mohiuddin-Jacobs, V. Petkov, S. J. L. Billinge, and S. Kycia, Phys. Rev. B **63**, 205202 (2001).
[16] P. F. Peterson, M. Gutmann, Th. Proffen, and S. J. L. Billinge, J. Appl. Crystallogr. **33**, 1192 (2000).
[17] I.-K. Jeong, J. Thompson, Th. Proffen, A. M. P. Turner, and S. J. L. Billinge, J. Appl. Crystallogr. **34**, 536 (2001).
[18] Th. Proffen and S. J. L. Billinge, J. Appl. Crystallogr. **32**, 572 (1999).
[19] B. E. Warren, *X-Ray Diffraction* (Dover, New York, 1990).
[20] J. S. Chung and M. F. Thorpe, Phys. Rev. B **55**, 1545 (1997).
[21] D. C. Koskenmaki and J. K. A. Gschneidner, *Handbook on the Physics and Chemistry of Rare Earths* (North-Holland, Amsterdam, 1978), Chap. 4.
[22] C. Stassis, T. Gould, O. D. McMasters, K. A. Gschneidner, and R. M. Nicklow, Phys. Rev. B **19**, 5746 (1979).

[23] M. Born and K. Huang, *Dynamical Theory of Crystal Lattices* (Oxford University Press, London, 1954).
[24] C. H. Booth, F. Bridges, E. D. Bauer, G. G. Li, J. B. Boyce, T. Claeson, C. W. Chu, and Q. Xiong, Phys. Rev. B **52**, R15 745 (1995).
[25] M. F. Thorpe (private communication).
[26] *Metalle: Phononenzustande, Elektronenzustande und Fermiflachen*, edited by P. H. Dederichs, H. Schober, and D. J. Sellmyer, Landolt-Börnstein, New Series, Group III, Vol. 13a (Springer, New York, 1981).
[27] P. Debye, Ann. Phys. (Leipzig) **39**, 789 (1912).
[28] G. Beni and P. M. Platzman, Phys. Rev. B **14**, 1514 (1976).
[29] E. Sevillano, H. Meuth, and J. J. Rehr, Phys. Rev. B **20**, 4908 (1979).
[30] W. Bohmer and P. Rabe, J. Phys. C **12**, 2465 (1979).
[31] R. J. Birgeneau, J. Cordes, and A. D. B. Woods, Phys. Rev. **136**, A1359 (1964).
[32] N. W. Ashcroft and M. D. Mermin, *Solid State Physics* (Holt, Rinehart and Winston, New York, 1976), Chaps. 28 and 29.
[33] V. Petkov, I.-K. Jeong, J. S. Chung, M. F. Thorpe, S. Kycia, and S. J. L. Billinge, Phys. Rev. Lett. **83**, 4089 (1999).
[34] A. A. Maradudin and P. A. Flinn, Phys. Rev. **129**, 2529 (1963).
[35] G. A. Wolfe and B. Goodman, Phys. Rev. **178**, 1171 (1969).
[36] C. J. Martin and D. A. O'Connor, Acta Crystallogr., Sect. A: Cryst. Phys., Diffr., Theor. Gen. Crystallogr. **34**, 500 (1978).
[37] C. J. Martin and D. A. O'Connor, Acta Crystallogr., Sect. A: Cryst. Phys., Diffr., Theor. Gen. Crystallogr. **34**, 505 (1978).
[38] A. C. Lawson, A. Williams, and M. S. Wire, J. Less-Common Met. **142**, 177 (1988).
[39] K. Nicolaus, J. Neuhaus, W. Petry, and J. Bossy, Eur. Phys. J. B **B21**, 357 (2001).
[40] G. Dalba, P. Fornasini, F. Rocca, and S. Mobilio, Phys. Rev. B **41**, 9668 (1990).
[41] P. Pavone, Ph.D. thesis, SISSA ISAS, 1991.